Journal of Statistical Physics, Vol. 49, Nos. 1/2, 1987

Anomalous Diffusion and Continuum Percolation

N. Wagner[1] **and I. Balberg**[1]

Received March 23, 1987

Anomalous diffusion for continuum percolation is simulated by considering systems of randomly distributed circles and spheres. Universal behavior is obtained for the case of equal local conductances and nonuniversal behavior for diverging distributions of the local conductances. Diffusion in the continuum has a behavior consistent with that of other transport properties in the continuum. In addition, the results suggest that different algorithms for diffusion, which differ only in the random walker sitting times, are equivalent.

KEY WORDS: Diffusion; anomalous diffusion; percolation; continuum percolation; random walk; conductivity exponent; Monte Carlo; universality; nonuniversality; distribution of conductances; myopic ant; blind ant; termite diffusion.

1. INTRODUCTION

Recently, there have been many Monte Carlo studies of diffusion in percolating lattice networks.[1–5] It seems then of interest to try to describe the diffusion process on continuum networks and to find its critical behavior. The conspicuous features that specify the percolating continuum networks in comparison with lattice networks are the unfixed number of possible connecting bonds per site (or per object), the variation of the bond length, and the local variation in the bond direction. Since the "macroscopic" isotropy of the system ensures that the last feature will be unimportant in "macroscopic" samples, we have to consider the other two features. In particular, we know that the local properties of the bond strength determine the critical behavior of the transport properties of the system.[6–11] On the other hand, the relatively wide distribution of the number of bonds per site (or per object), which is of particular importance in the diffusion process, has not been considered previously.

[1] Racah Institute of Physics, Hebrew University, Jerusalem 91904, Israel.

0022-4715/87/1000-0369$05.00/0

Following these considerations, we have simulated a diffusion process on systems of randomly placed circles and spheres and have determined the anomalous diffusion exponent k in the appropriate regimes. To check the effect of the above mentioned features, we had to modify previous lattice algorithms,[1,12,13] as will be discussed in Sections 2 and 3. Correspondingly, we started with a diffusion process on a system with a continuum geometry but fixed bond strength (Section 2), and then introduced the effect of bond strength variation (Section 3) into the system. The present results (Section 4) show that the statistical–structural differences between the lattice and the continuum are not manifested by a different universality class for the diffusion process. Furthermore, the variations in the local transport properties affect the diffusion process in the manner to be expected from the scaling theory of anomalous diffusion. Our results further indicate (Section 5) a general property of the diffusion process in a disordered system, i.e., that the critical behavior is dependent only on the relative "hopping" probability to adjacent sites and is independent of the "sitting time" on the site.

2. DIFFUSION IN CONTINUUM SYSTEMS

Diffusion in the continuum may differ from lattice diffusion as a result of the following inherent differences between putting objects in the continuum and placing sites on a lattice: (1) the centers of the objects do not have discrete "addresses," but can lie anywhere within the continuum space; (2) the coordination number of a lattice represents the maximum number of nearest neighbors of any lattice site, while there is (in an infinite sample) no upper limit to the possible number of intersecting neighbors of a given object in the continuum. Our new algorithm is designed to account for these differences. For simplicity it is presented here in its two-dimensional form. The extension to higher dimensions is straightforward.

We begin by randomly placing circles of fixed radius on a square of unit area (henceforth all lengths referred to will be in units of this square's edge). The x and y coordinates of a circle center are chosen by a random number generator, and each circle is numbered according to the order in which it is placed. As each circle is placed, we also determine whether its center lies within a central "window" (whose sides are of length 0.2) or whether its center lies within the boundary region at the edges of the unit square. A typical (though small) sample generated by the computer is shown in Fig. 1.

In our computer program, each circle is checked for overlap with all previous circles. A matrix is built where the elements in row i give the circles that intersect circle i. Simultaneously, we use a variation of the

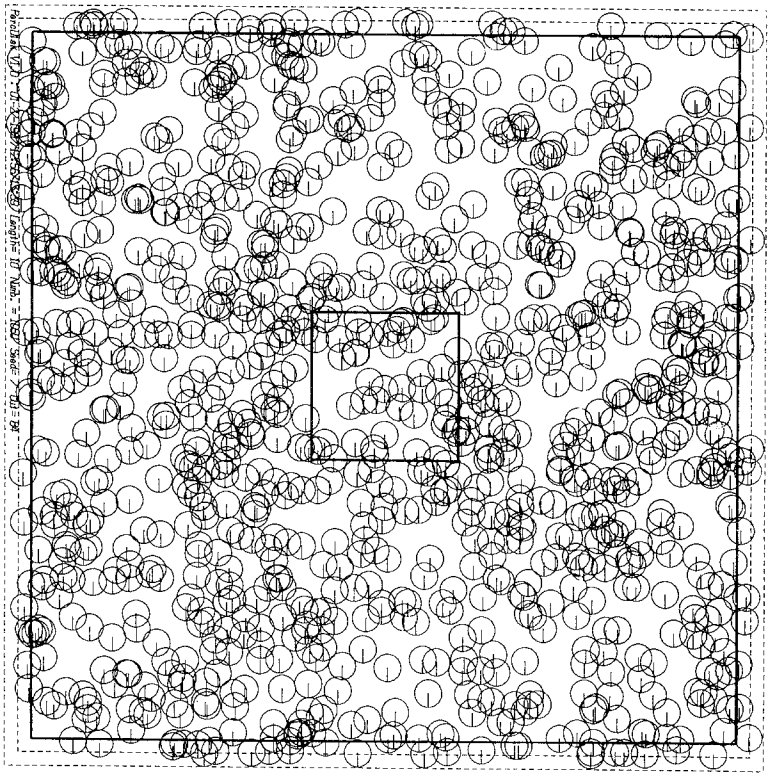

Fig. 1. A configuration of circles describing the samples on which the diffusion computations were carried out. The central window (inner square) is the region where a random walk begins, and the boundary region (outer square) is where a random walk ends. This picture shows 1000 circles, while the samples used for the computations were of about 10,000 circles (or spheres).

Hoshen–Kopelman algorithm[14] to check for percolation (along one of the unit square axes). This procedure is continued until the percolation threshold is reached. At this point we begin to simulate diffusion. A starting circle whose center is located within the central "window" is chosen randomly, its position recorded, and its center set as the local origin, where our random walker "ant" starts its random walk. The ant then selects a new circle (one of the intersecting circles) or remains on the same circle, in a process to be described subsequently. When the ant hops to the center of a selected circle (whether or not the ant has actually moved), a unit of time is recorded. The above process is repeated from the next circle and continued until the clock reaches a preset value. After each time unit we record the distance of the ant from the local origin, R. This procedure, using a new starting circle chosen randomly, is repeated for a preset number of ants.

The actual process of hopping from a given circle to a new circle follows the "blind ant"[1] algorithm. Here, however, as pointed out above, we do not have an upper limit to the number of intersecting neighbors for a given circle, so we have to modify the above common algorithm. We have done that by using M, the maximum number of intersections per circle in the particular sample studied, as a normalizing constant.[15] Thus, if a given circle has N intersecting neighbors, the ant will hop to each of these neighbors with probability $1/M$ and remain in place with probability $1-N/M$.

We note that despite the similarity of the diffusion process described by the present algorithm and the corresponding process on lattices, the respective results may differ due to the differences mentioned above. In addition, for our continuum algorithm, the ant remains in place much longer, on the average, than its lattice counterpart. This is because M is uncharacteristically high (in general, $N \ll M$), while the lattice coordination number is not uncharacteristically high (zp_c is of the order of z, where z is the lattice coodination number and p_c is the critical occupation probability). Thus, our continuum blind ant moves more slowly than the lattice blind ant, and perhaps should be nicknamed the "lazy blind ant." The other extreme, i.e., when the ant never chooses to stay on the same site (or circle), is known as the "myopic ant."[1] To check further the effect of the sitting time, we also used the myopic ant algorithm (hop probability $1/N$) in our continuum systems.

In an attempt to approximate properly a random walk on an infinite network while having a finite sample, we require the following: all random walks must begin from one of the circles located within the central window and may not cross the boundary (we use no periodic boundary conditions, which are potentially biasing[4] and are difficult to establish for the continuum). The boundary region at the edges has a width equal to a circle radius; a circle in this region could conceivably intersect with a circle outside our sample, i.e., with a circle in the infinite network not represented in our finite sample. Therefore, when the ant enters the boundary region, the walk is stopped, and the time of "falling off the edge" (i.e., touching the boundary) is recorded. Any data for later times cannot be relied upon. By starting the walks only from the central window (which is an unbiased representative "cut" from the entire sample) we ensure that our walks are sufficiently long. Additionally, any ant beginning in an isolated circle (one that intersects no others) just stays at the same place the entire time. In such cases we save computer time by skipping the entire diffusion process for this walk.

After the diffusion process is repeated for a preset number of ants, we build a new random sample and repeat the entire process. Finally we

average together the results, i.e., the square of the distances R^2 from the respective local origins, for all the ants and samples, to get the $\langle R^2 \rangle$ displacement as a function of time t.

3. DIFFUSION IN A CONTINUUM NETWORK WITH VARYING LOCAL CONDUCTANCES

Our algorithm for diffusion in a network of varying local conductances was implemented in the continuum by following the same general outline as the algorithm described in Section 2. For this case, however, we attribute a given conductance to every pair of intersecting circles. Our previous algorithm can then be thought of as the specific case where all the conductances between intersecting circles are equal.

As each circle is checked for intersection with previously placed circles, we select a value for the conductance between the intersecting circles and store it in a second matrix. Thus, in addition to the first matrix, which lists, in row i, the circles intersecting circle i, this parallel matrix gives, in row i, the corresponding conductance values. The necessity of computing and storing a second large matrix is one aspect of the greater computational difficulty of this second algorithm.

The diffusion process itself is similar to that of the previous case, except for the "moody" movement of the ant. At each "tick" of the clock, instead of selecting a neighboring intersecting circle with probability $1/M$, the blind ant selects a given circle with probability g_j/M, where g_j $(0 \leqslant g_j \leqslant 1)$ is the conductance between the ant's circle and circle j. Hence, the ant will remain on the same circle with probability $1 - \sum g_m/M$, where the sum is over all intersecting (neighboring) circles. (In contrast, the myopic ant select a given j with probability $g_j/\sum g_m$, and never remains on the same circle.)

Our algorithm is, in a way, a generalization of previous "termite" algorithms,[12,13] which describe diffusion in media containing two components of nonequal conductivity. In particular, it is similar to the so-called "Boston Termite 1."[13]

The other details of the diffusion process, statistics, and acquisition of data are as described in Section 2.

In order to check the effect of bond strength variation, we have used the random distribution[6,7]

$$P(g)\, dg = (1 - \alpha)\, g^{-\alpha}\, dg \tag{1}$$

where $0 \leqslant g \leqslant 1$ and α is a constant $(\alpha < 1)$. This distribution is selected since it is well known to yield nonuniversal values for the transport

exponents[6–11] and since it has been shown[5] to yield the corresponding nonuniversal anomalous diffusion exponents on lattices (see below). Hence, applying this distribution to the continuum geometry used in the present paper is expected to account for the diversity of the objects' environments (see Section 1) that can be found in real continuum systems. It is to be pointed out that particular physical situations may suggest other conductance distributions which can be investigated using the present algorithm.

If $P(g)$ does not diverge as $g \to 0$, we expect a behavior similar[7] to the one discussed in Section 2. For the distribution of interest, which is given by Eq. (1), each conductance value is computed by looking at the cumulative distribution function[16]:

$$I(g) = \int_0^g P(g')\, dg' = g^{1-\alpha} \tag{2}$$

where I is chosen randomly between 0 and 1, and g is then simply given by

$$g = I^{1/(1-\alpha)} \tag{3}$$

4. RESULTS

We used the algorithms described in Sections 2 and 3 to simulate diffusion in the anomalous regime, i.e., when the system is at the percolation threshold and the region visited by the ant is self-similar ($\xi \gg L$, where ξ is the correlation length and L is the sample size). For each of the four cases to be considered, ten different configurations (samples) were used, and on each configuration 1000 ants were sent in the manner described above. From all these data the average $\langle R^2 \rangle$ was determined as a function of time. Using two-dimensional (three-dimensional) systems, we set the fixed radius of each circle (sphere) at 0.006 (0.02). This choice yielded approximately 10,000 circles (spheres) at the percolation threshold (the exact value varied slightly with each configuration). Note that the sample size L is essentially the inverse of the above fixed radius. Hence, even though the number of objects is the same, the three-dimensional samples are about three times smaller than the two-dimensional samples.

Our results, to be presented below, are given by log–log plots of $\langle R^2 \rangle$ versus walking time t. Following the definition[1] of the anomalous diffusion exponent k

$$\langle R^2 \rangle \propto t^{2k} \tag{4}$$

we obtained the value of $2k$ directly from the slope of the log–log plot. Then, using the scaling relation of anomalous diffusion[1]

$$2k = (2\nu - \beta)/(2\nu - \beta + \mu) \tag{5}$$

we also determined the value of the conductivity exponent μ. This was done by using the universal values[1] of the correlation length exponent ν and the percolation cluster exponent β:

$$\nu = \begin{cases} 4/3 & (2D) \\ 0.9 & (3D) \end{cases}, \qquad \beta = \begin{cases} 5/36 & (2D) \\ 0.4 & (3D) \end{cases} \tag{6}$$

Our approach appears to be justified (see Section 5), since it has already been shown[17-19] that the statistical and geometrical critical exponents obey lattice/continuum universality.

Figure 2 shows the results for the two-dimensional case of random circles. To obtain the value of $2k$, we have followed Havlin and Ben-Avraham,[3] who demonstrated that the correct value is obtained by taking the slope at asymptotically large t. This is consistent with the correction-to-scaling relation proposed by Pandey *et al.*[4]:

$$\bar{R} \equiv \langle R^2 \rangle^{1/2} = t^k (a - b/t^l) \tag{7}$$

where a, b, and l are constants. Since the samples are finite, one cannot take as high a t as one wishes, due to the falling-off-the-edge effect described in Section 2 (the downturn for $t > 10^4$ in Fig. 2 is due to this effect). Correspondingly, we recorded the time of falling for each ant and

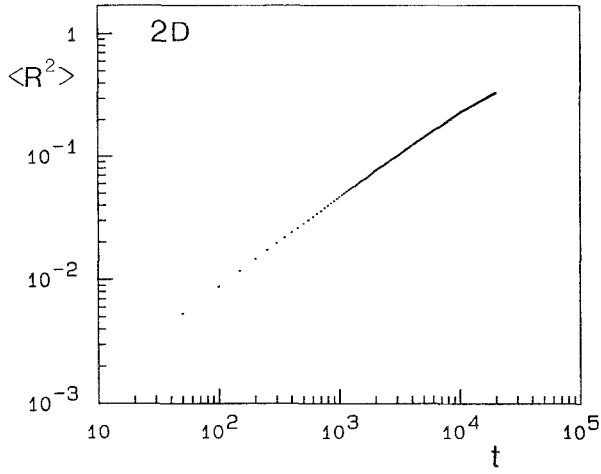

Fig. 2. The dependence of the average $\langle R^2 \rangle$ (where R is the distance traveled by the diffusing ant), on the number of step attempts t in samples of the type described in Fig. 1. The systems are exactly at their percolation threshold.

did not consider the slope beyond this time. In the present case we took the slope in the time regime $10^3 < t < 10^4$, obtaining

$$2k = 0.66 \pm 0.03, \qquad \mu = 1.3 \pm 0.2$$

These values for k and μ are consistent with results obtained from simulations of two-dimensional lattice diffusion.[4] Furthermore, the value obtained for μ is consistent with those obtained using other Monte Carlo procedures,[1] such as the transfer matrix method for lattices[20] and the matrix inversion method for the continuum.[21]

Figure 3 shows the $\langle R^2 \rangle$ versus t results for the two-dimensional case with a conductance value distribution. The conductors network is determined by the bond configuration, which results from the intersections of the circles in a sample such as the one shown in Fig. 1. The local conductance values are chosen using the distribution given by Eq. (1) for $\alpha = 0.8$. Following the considerations used in taking the $\langle R^2 \rangle$ versus t slope in Fig. 2, we determine the value of the slope in the present case in the time region $10^5 < t < 10^6$. These relatively much larger times (in comparison with those in the single-value-conductance network, Fig. 2) are due to the many poor conductors in the present network; the diffusion process is slowed down, and the time of falling off the edge is prolonged considerably. Using the above procedure, we obtain for this case

$$2k = 0.41 \pm 0.02, \qquad \mu = 3.6 \pm 0.3$$

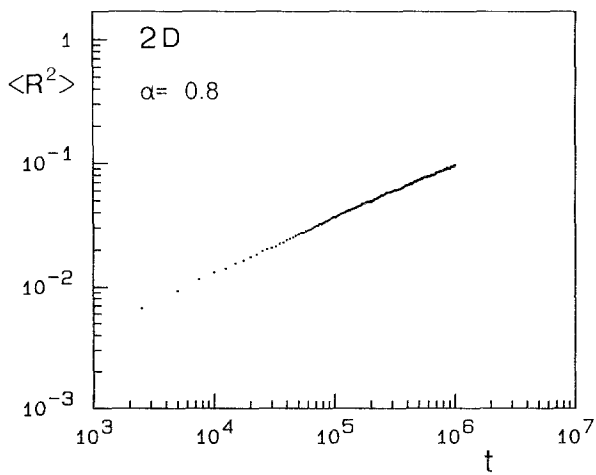

Fig. 3. Same as Fig. 2, except that the conductance distribution given by Eq. (1) has been introduced.

This "nonuniversal" decrease of the anomalous diffusion exponent is consistent with the predicted increase of the conductivity exponent[6,8,9] for the distribution used if one assumes that the scaling relation (5) holds also for the present case. On the other hand, the value obtained for μ by using this relation is somewhat lower than expected. This is borne out by the fact that the value of μ is predicted to be within the interval[7]

$$(d-2)\nu + 1/(1-\alpha) \leqslant \mu \leqslant (\mu_{\text{univ}} - 1) + 1/(1-\alpha) \tag{8}$$

where d is the dimensionality of the system and μ_{univ} is the appropriate "universal" value.[1] In two dimensions (where $\mu_{\text{univ}} = 1.3$) this implies that for $\alpha = 0.8$ one should find $5.0 \leqslant \mu \leqslant 5.3$. Clearly, our value for μ is smaller than these values. We shall further discuss this deviation below.

Figure 4 shows the results obtained for a system of spheres in the three-dimensional continuum. In three dimensions our samples are smaller (see Section 4) and the diffusivity is larger than in two dimensions, because the cluster backbone is less "blobby," leading to a more "efficient" diffusion process. The latter effect will be enhanced for the "lazy blind ant," since M in three dimensions is smaller than M in two dimensions. This result is simply due to the fact that in general there is a smaller critical number of bonds per site in the three-dimensional case. Hence, the time of falling-off-the-edge is much shorter here than for its two-dimensional counterpart. Correspondingly, to find $2k$ in the three-dimensional case, we had to take the slope in the region $10^2 < t < 10^3$. Following the above discussion, one

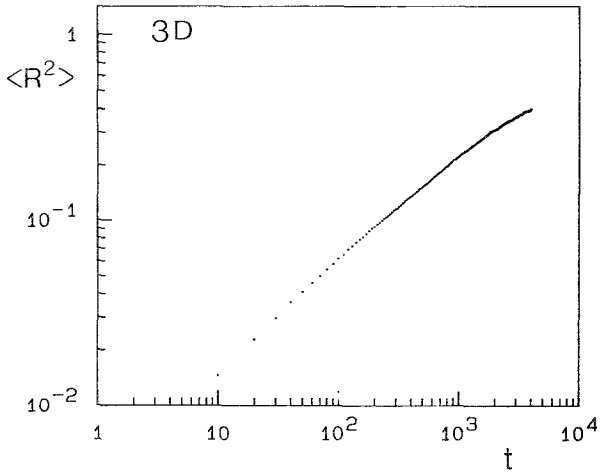

Fig. 4. Plot of $\langle R^2 \rangle$ versus t for a three-dimensional systems of spheres when the systems are at the percolation threshold.

expects the three-dimensional $2k$ values to be less accurate and farther removed from the "correct" asymptotic value than the two-dimensional values. Furthermore, Pandey *et al.*[4] predict that the correction term in Eq. (7) is larger in three dimensions than in two, which would require one to compute the three-dimensional slope at even higher t values than in the two-dimensional case. In view of this, it is apparent that in the three-dimensional case it is much more likely that we have to account for the finite times of the actual measurement. Therefore, we followed Ref. 4 in determining $2k$ by extrapolating to infinite time. For this purpose, we determined the slope at various times. The corresponding value of the slope yields an "effective value" $2k_{\text{eff}}$ at a given time. Now, following Eq. (7), i.e., plotting the values of $2k_{\text{eff}}$ as a function of t^{-l}, one expects to get the extrapolated value of $2k$. If this correction term is proper, we should get a straight line [note that

$$k_{\text{eff}} = d(\log \bar{R})/d(\log t) = k + (lb/a)t^{-l}]$$

so that the vertical axis intercept will yield the "correct" or "asymptotic" value of $2k$. By following the conjecture[4] that b/t^l (the leading correction term) varies in three dimensions as $1/\bar{R}$, one expects that $l \approx k$. Hence, we plotted $2k_{\text{eff}}$ (computed at various points from $t = 10$ to $t = 1000$) as a function of t^{-l} for various values of l. This procedure was continued until the obtained value of k was consistent with the $l \approx k$ condition. In our case this was found for $l = 0.20$. As shown in Fig. 5, the straight line

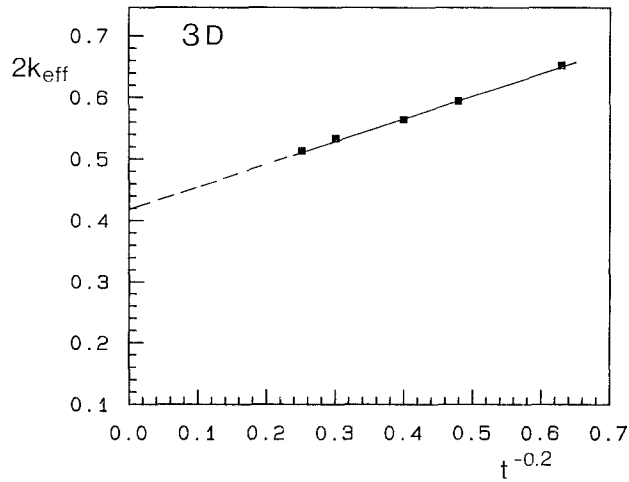

Fig. 5. Plot of $2k_{\text{eff}}$ as a function of time for the results plotted in Fig. 4. The $t \to \infty$ asymptotic limit yields the "correct" value of $2k = 0.42$ (see text).

approximation appears to be quite good for the l value chosen, yielding the extrapolated values

$$2k = 0.42 \pm 0.01, \qquad \mu = 1.9 \pm 0.1$$

These results for three dimensions are again very close to previously reported values for k (using a similar procedure[4]) and for μ on lattices.[1,22]

In Fig. 6 we show our results for the $\langle R^2 \rangle$ dependence on t as obtained on a three-dimensional system of spheres, where variable-value conductances are attached to intersecting spheres. As in the two-dimensional case, we used the above distribution [Eq. (1)] with $\alpha = 0.8$. Again, the slowing of the diffusion process causes the falling-off-the-edge effect to be delayed, and we got reliable results for up to $t = 10^5$. Using the correction considered above, i.e., that $b/t^l \propto 1/\bar{R}$, we repeated the same procedure for the determination of the asymptotic k value. This time the value $l = 0.10$ yielded a value of k consistent with $l \approx k$. The results obtained by plotting $2k_{\text{eff}}$ as a function of $t^{-0.10}$ were

$$2k = 0.22 \pm 0.02, \qquad \mu = 5.0 \pm 0.6$$

The latter result is to be compared with the expectation from Eq. (8), when one considers the three-dimensional known values[1] of $\nu = 0.9$ and $\mu_{\text{univ}} = 2.0$. This consideration, for $\alpha = 0.8$, implies that $5.9 \leqslant \mu \leqslant 6.0$. Again, our result is close to, but slightly lower than, that suggested by Eq. (8).

Using a procedure similar to that described for three dimensions, we can also extrapolate to infinite times in two dimensions. In this case, however, the relation $b/t^l \propto 1/\bar{R}$ does not seem to hold.[4] One may follow

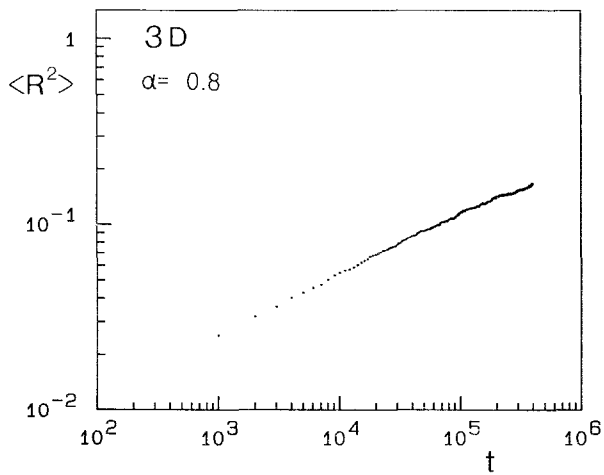

Fig. 6. Same as Fig. 4, except that the conductance distribution given by Eq. (1) has been introduced.

then Ref. 4 in assuming that $l_2 \approx 2l_3$, where l_2 and l_3 refer to the respective correction-to-scaling exponents in two and three dimensions. Following this assumption for the analysis of our results for the two-dimensional system of random circles, we plotted $2k_{\text{eff}}$ versus $t^{-0.45}$ and obtained

$$2k = 0.64 \pm 0.01, \qquad \mu = 1.4 \pm 0.1$$

The fact that these values are, within the error bars, the same as the uncorrected results given above (i.e., that the correction did not improve the results) shows that our two-dimensional system is a good (to the above accuracy) approximation of an infinite system.

For the two-dimensional varying-conductance case with $\alpha = 0.8$, we followed a similar procedure, and plotted $2k_{\text{eff}}$ versus both $t^{-0.20}$ and $t^{-0.25}$. The two plots yielded essentially the same extrapolated values for $2k$. The "corrected" results can be summarized then by

$$2k = 0.35 \pm 0.02, \qquad \mu = 4.7 \pm 0.4$$

While this corrected value for μ is closer to the predictions of Eq. (8) than the (large-t) unextrapolated result given above, it is still slightly lower than expected. The improvement here, in comparison with the single-value-conductance case, is (as will be discussed in Section 5) a result of the larger deviation from "infinite sample" conditions in the present case.

We also-simulated "myopic ant" (zero sitting time) anomalous diffusion[1,23] for the same four cases discussed above, and obtained similar results (within the range of error). This is consistent with previous results on lattices, which concluded that the myopic and the blind ant belong to the same universality class.[23,24] Our results show, however, that this is also true for the varying-conductances case. This agreement is not automatically expected, since the myopic ant (which hops at every time step) effectively renormalizes the hopping probabilities at each step, thus moderating the effects of the "weak bonds" that play such a crucial role in the nonuniversal behavior.[7]

5. DISCUSSION

The values obtained in Section 4 for the anomalous diffusion exponents both in two dimensions ($2k = 0.66 \pm 0.03$) and in three dimensions ($2k = 0.42 \pm 0.01$) show that diffusion in a continuum geometry belongs to the same universality class as diffusion on lattices. Furthermore, the fact that the corresponding μ values ($\mu = 1.33 \pm 0.3$ and $\mu = 1.9 \pm 0.1$) are equal to those previously obtained by other methods on lattices and continuum systems indicates that the scaling relation (5) also holds in the continuum.

The results, following the application of a conductance distribution (which appears to be more natural in continuum systems; see Section 1), are also in accord with the above conclusion in the sense that the nonuniversality is also the same for lattice and continuum systems. It is not affected by the number-of-neighbors distribution, but is affected by the bond strength distribution. This is borne out by the fact that if one considers diffusion on a lattice geometry, as was done by Bunde *et al.*,[5] or if one considers a continuum geometry, as was done in the present work, one obtains the same results.

We noted in Section 4 that assuming the existence of the scaling relation (5) for the case of a conductance distribution with a nonuniversal μ has yielded, in both the two-dimensional and three-dimensional computations, conductivity exponents slightly lower than the lower bounds predicted by Eq. (8). In view of the data obtained on lattices, this deviation appears to be quite general. For example, for $\alpha = 3/4$, Bunde *et al.*,[5] by applying the scaling relation (5), obtained $\mu = 3.9$ in 2D, while for $\alpha = 5/7$, Murat *et al.*,[11] using another approach (the transfer matrix algorithm), obtained $\mu = 4.1$ in 3D. These values fall below the lower bounds predicted by Eq. (8) ($\mu = 4.0$ and $\mu = 4.4$, respectively). In fact, the three previous simulations[5,10,11] in which a varying-conductance network was considered reveal the following trend: for small values of α, μ is quite close to the original theoretical prediction of Kogut and Straley,[6]

$$\mu_{KS} = (\mu_{univ} - 1) + 1/(1 - \alpha) \tag{9}$$

but as α is increased, the "experimental" μ does not increase as dramatically as μ_{KS}. The generality of the above discrepancy and trend indicate a finite-size effect; as α increases, the sample becomes effectively too small to simulate properly the specific distribution, and hence a much larger sample is needed to equivalently approximate (say, for our $\alpha = 0.8$ case) an infinite sample. In other words, if one stays with the same sample size (number of objects) but increases α, one reduces the statistical quality of the sample. The effect of the finite size is well known to reduce the conductivity exponent, since the critical resistivity divergence becomes weaker.

An interesting observation is that the critical behavior of anomalous diffusion is not affected by the time interval during which the ant stays at a given site or object. Hence the myopic ant, the blind ant, and our "lazy blind ant" all show the same universal behavior. Essentially this observation was made before for lattices by the comparison of the first two cases.[23] The extension to the third case considered here is not obvious, because the sitting time here, while relatively large, is weakly controlled by the local environment. Furthermore, in the case of a conductance dis-

tribution, the effective reduction of the hop probability may appear to be stronger in the case of the "lazy blind ant" (where a singly connected bond has a hop probability g_j/M) in comparison with that of the myopic ant (hop probability g_j). We may conclude, then, that it is the connectivity of the system that determines the critical behavior of the diffusion process. Differences in the sitting times do not affect the universality. On the other hand, differences in the hopping times to different neighbors (different bond strengths) yield the "conventional" nonuniversal behavior.

ACKNOWLEDGMENTS

We would like to thank S. Havlin, J. Kertsz, and S. Shickman for helpful discussions and suggestions. One of us (N. W.) gratefully acknowledges the hospitality of R. B. Laibowitz and co-workers at the IBM Thomas J. Watson Research Center.

REFERENCES

1. D. Stauffer, *Introduction to Percolation Theory* (Taylor & Francis, London, 1985).
2. C. D. Mitescu and J. Roussenq, *Ann. Israel Pys. Soc.* **5**:81 (1983).
3. S. Havlin and D. Ben-Avraham, *J. Phys. A* **16**:L483 (1983).
4. R. B. Pandey, D. Stauffer, A. Margolina, and J. G. Zabolitzky, *J. Stat. Phys.* **34**:427 (1984).
5. A. Bunde, H. Harder, and S. Havlin, *Phys. Rev. B* **34**:3540 (1986).
6. P. M. Kogut and J. P. Straley, *J. Phys. C* **12**:2151 (1979).
7. B. I. Halperin, S. Feng, and P. N. Sen, *Phys. Rev. Lett.* **54**:2391 (1985).
8. A. Ben-Mizrachi and D. J. Bergman, *J. Phys. C* **14**:909 (1981).
9. J. P. Straley, *J. Phys. C* **15**:2343 (1982).
10. P. N. Sen, J. N. Roberts, and B. I. Halperin, *Phys. Rev. B* **32**:3306 (1985).
11. M. Murat, S. Marianer, and D. J. Bergman, *J. Phys. A* **19**:L275 (1986).
12. F. Levyraz, J. Adler, A. Aharony, A. Bunde, A. Coniglio, D. C. Hong, H. E. Stanley, and D. Stauffer, *J. Phys. A* **19**:3683 (1986).
13. A. Bunde, A. Coniglio, D. C. Hong, and H. E. Stanley, *J. Phys. A* **18**:L137 (1985).
14. J. Hoshen and R. Kopelman, *Phys. Rev. B* **14**:3438 (1976).
15. S. Havlin, private communication.
16. D. E. Knuth, *The Art of Computer Programming*, 2nd ed., Vol. 2—*Seminumerical Algorithms* (Addison-Wesley, Reading, Massachusetts, 1981), pp. 116–117.
17. S. W. Haan and R. Zwanzig, *J. Phys. A* **10**:1547 (1977); T. Vicsek and J. Kertesz, *J. Phys. A* **14**:L31 (1981); E. T. Gawlinski and H. E. Stanley, *J. Phys. A* **14**:L291 (1981); J. Kertesz and T. Vicsek, *J. Phys. B* **45**:345 (1982).
18. A. Geiger and H. E. Stanley, *Phys. Rev. Lett.* **49**:1895 (1982).
19. I. Balberg and N. Binenbaum, *Phys. Rev. A* **31**:1222 (1985).
20. B. Derrida and J. Vannimenus, *J. Phys. A* **15**:L557 (1982).
21. I. Balberg, N. Binenbaum, and C. H. Anderson, *Phys. Rev. Lett.* **51**:1605 (1983).
22. B. Derrida, D. Stauffer, H. J. Herrmann, and J. Vannimenus, *J. Phys. Lett. (Paris)* **44**:L701 (1983).
23. E. Seifert and M. Suessenbach, *J. Phys. A* **17**:L703 (1984).
24. I. Majid, D. Ben-Avraham, S. Havlin, and H. E. Stanley, *Phys. Rev. B* **30**:1626 (1984).